Supplement of Nat. Hazards Earth Syst. Sci., 24, 2995–3012, 2024
https://doi.org/10.5194/nhess-24-2995-2024-supplement

Natural Hazards and Earth System Sciences
Open Access
EGU

Supplement of

Precursors and pathways: dynamically informed extreme event forecasting demonstrated on the historic Emilia-Romagna 2023 flood

Joshua Dorrington et al.

Correspondence to: Joshua Dorrington (joshua.dorrington@uib.no)

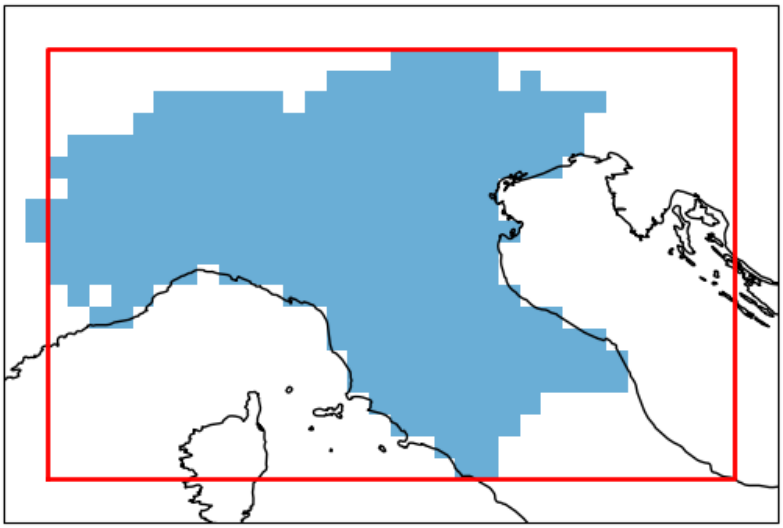

Figure S1. In blue, the 0.25 degree mask, used to spatially aggregate precipitation over North Italy. Lagrangian trajectories were started within the bounds of the red box spanning 7-15E, 42-47N.

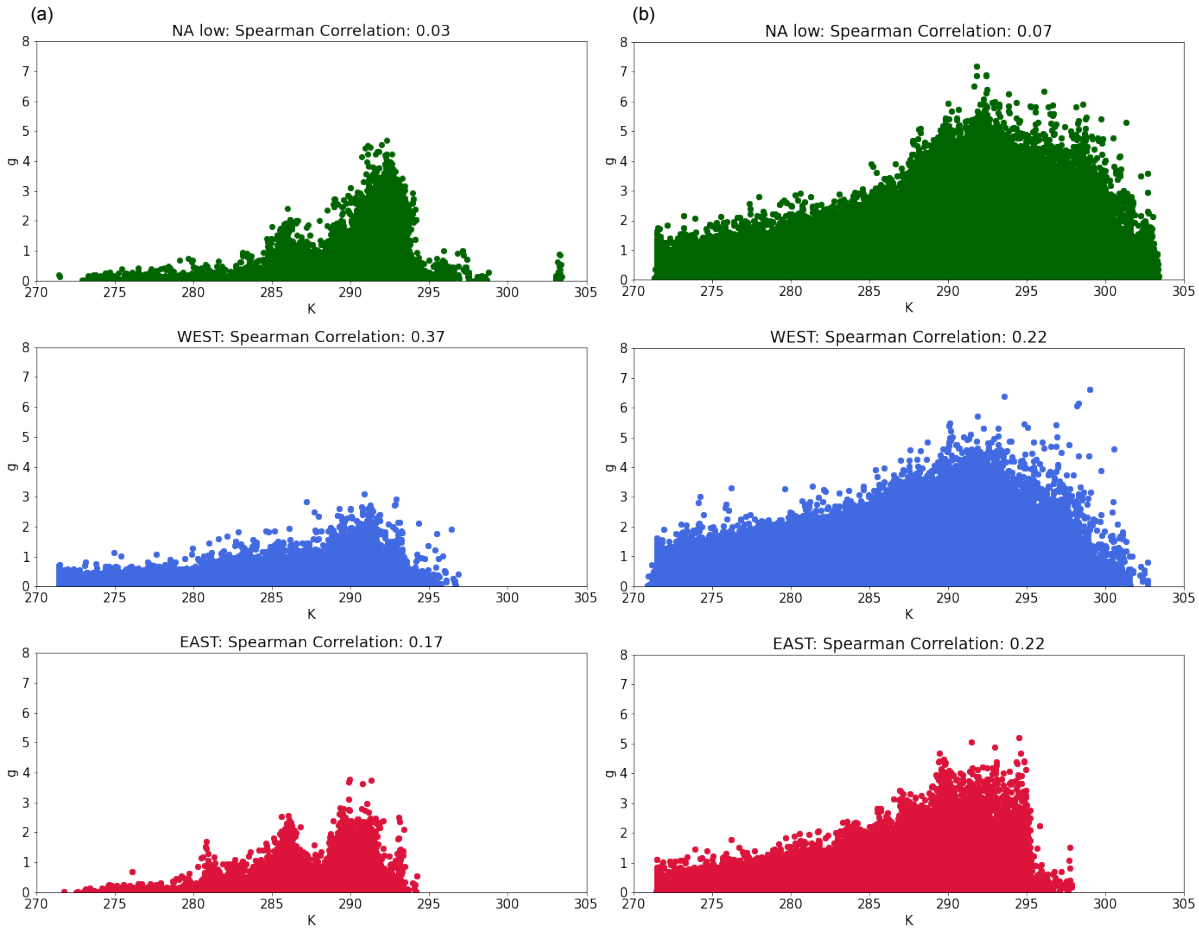

Figure S2. Scatter plot of moisture uptakes intensity (g) and the SST(K) experienced by air parcel during an uptake: Plots (a) and (b) represent data from NA low trajectories, (c) and (d) from WEST datasets, and (e) and (f) from EAST pathways. The first column presents data from a rainfall case study in May 2023, while the second column refers to the climatology of 66 events. Each plot is titled with its Spearman correlation coefficient, reflecting the correlation between SST and uptake intensity.

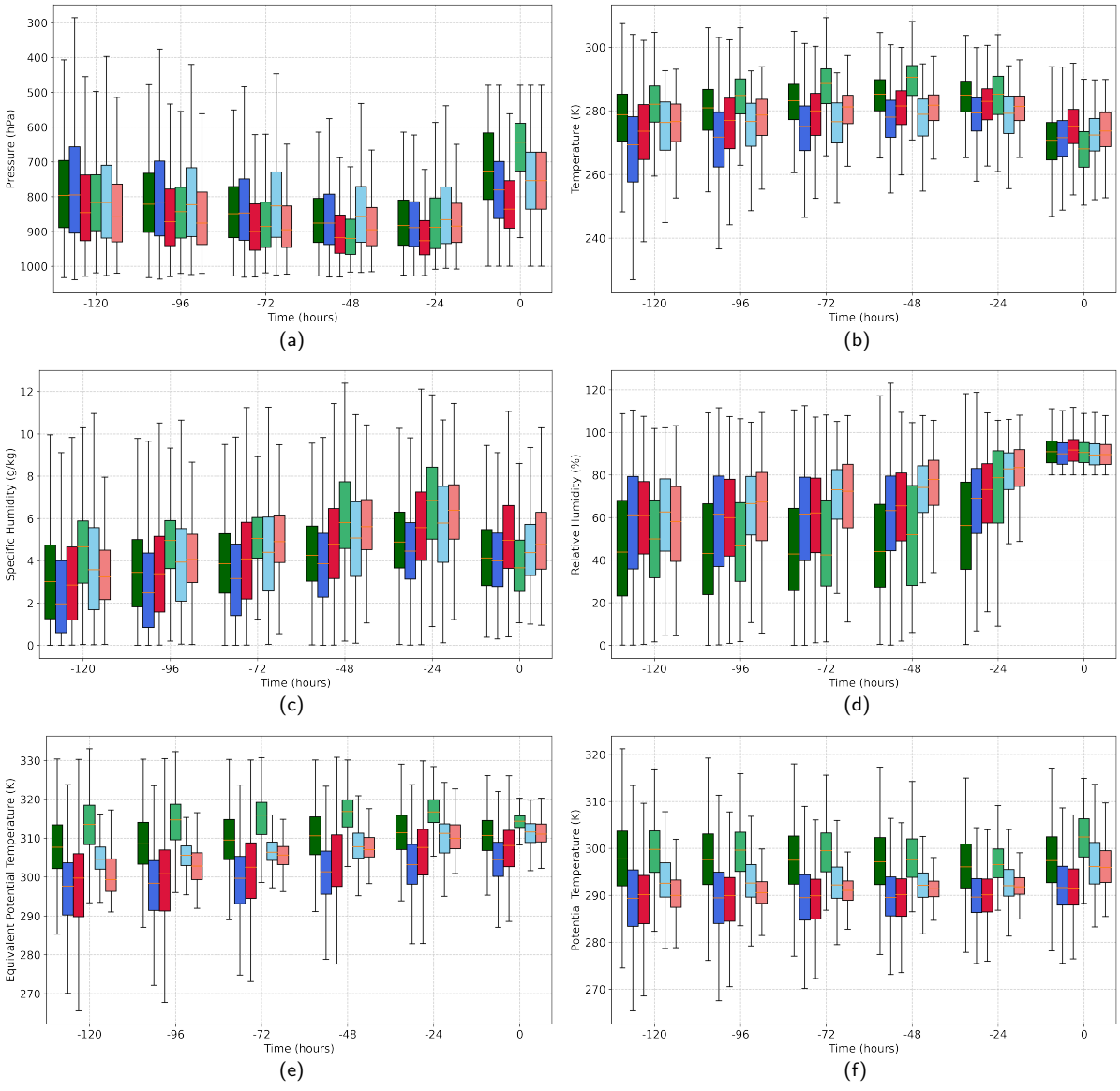

Figure S3. Boxplots showcasing properties ((a) pressure, (b) temperature, (c) specific humidity, (d) relative humidity, (e) equivalent potential temperature, (f) and potential temperature) of NAlow (dark and light green), WEST (dark and light red), and EAST (dark and light blue) trajectories for time steps -120h, -96h, -72h, -48h, -24h, 0h from the trajectory initiation, where dark colors represent climatology and light colors denote case study of May 2023.

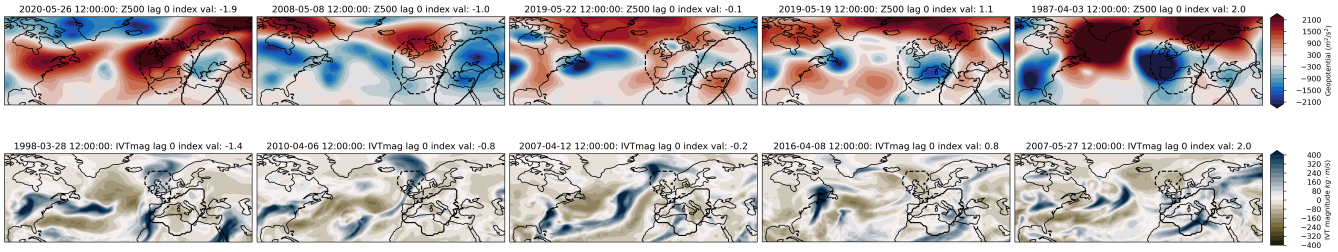

Figure S4. Randomly selected daily Z500 (top) and IVTmag (bottom) anomaly fields, with the bounds of the north Italy Z500/IVTmag lag 0 precursor patterns overlaid, and with the corresponding precursor activity index shown. These are included in order to provide some intuition to readers unfamiliar with the precursor approach. Activity indices are standardised to mean 0 and standard deviation 1. Large positive values indicate the presence of a rainfall-supporting large-scale flow and so an increased likelihood of an extreme rainfall event.

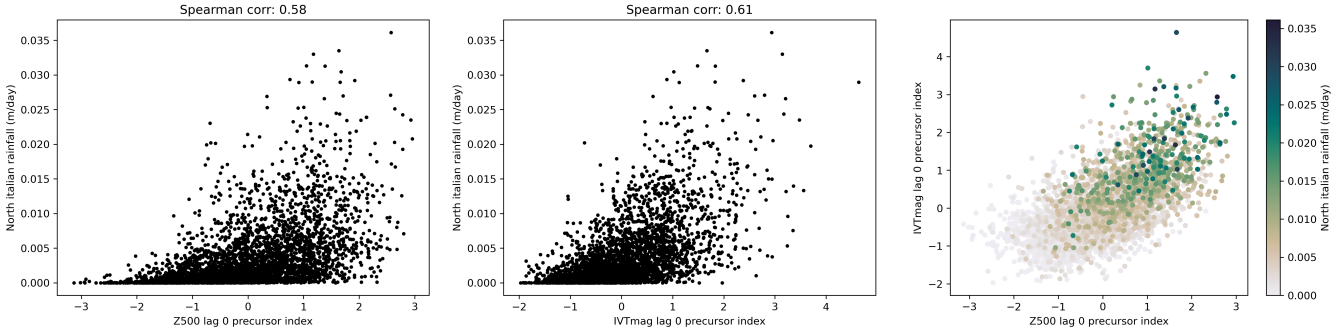

Figure S5. Left: A scatter plot of daily MAM Z500 lag 0 precursor activity indices against daily north Italian precipitation, over 1979-2021. Middle: Same for MAM IVTmag lag 0 precursor activity indices. Right: Covariation between IVTmag and Z500 lag 0 indices, with rainfall total shown in shading.

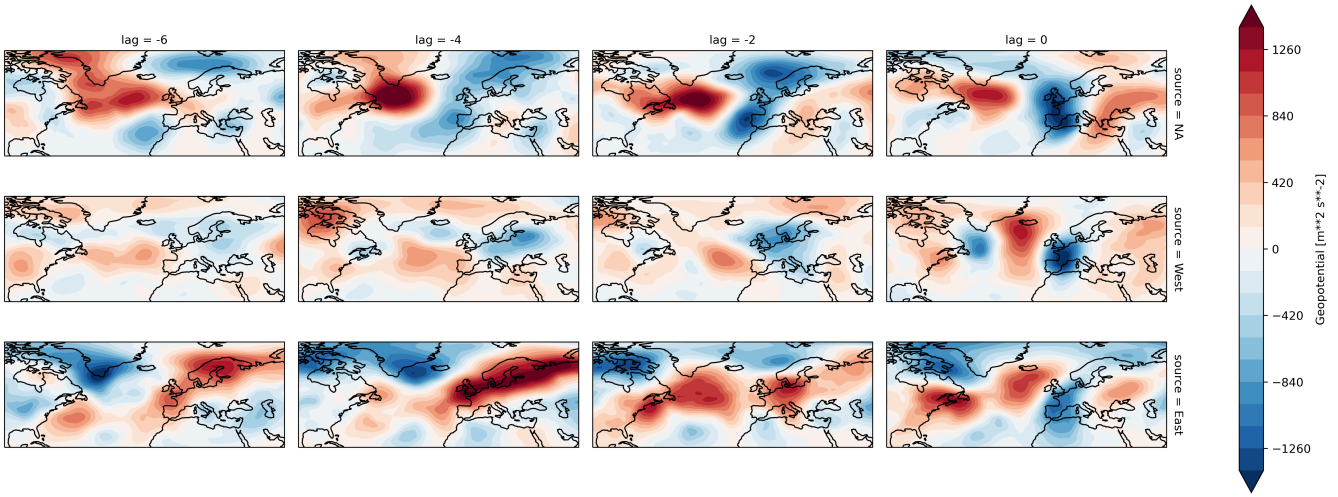

Figure S6. Lagged composites of Z500 anomalies, 6, 4, 2 and 0 days before rainfall events driven by each of the Lagrangian moisture pathways shown in main figure 1.

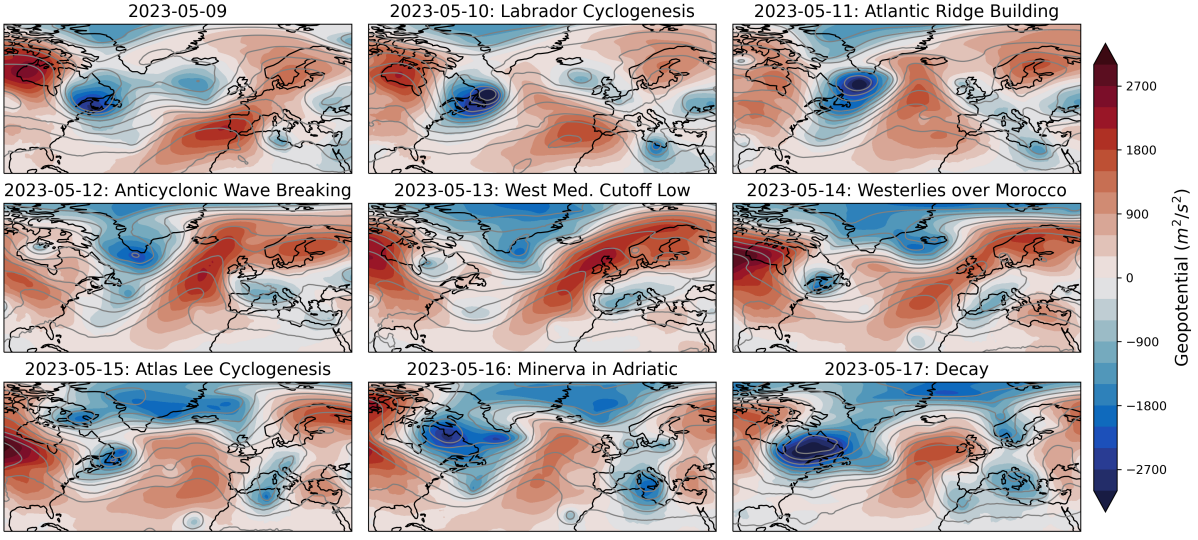

Figure S7. 500 hPa Geopotential anomalies (shaded) with full-field contours overlaid, showing the synoptic evolution leading up to storm Minerva and the case study extreme.

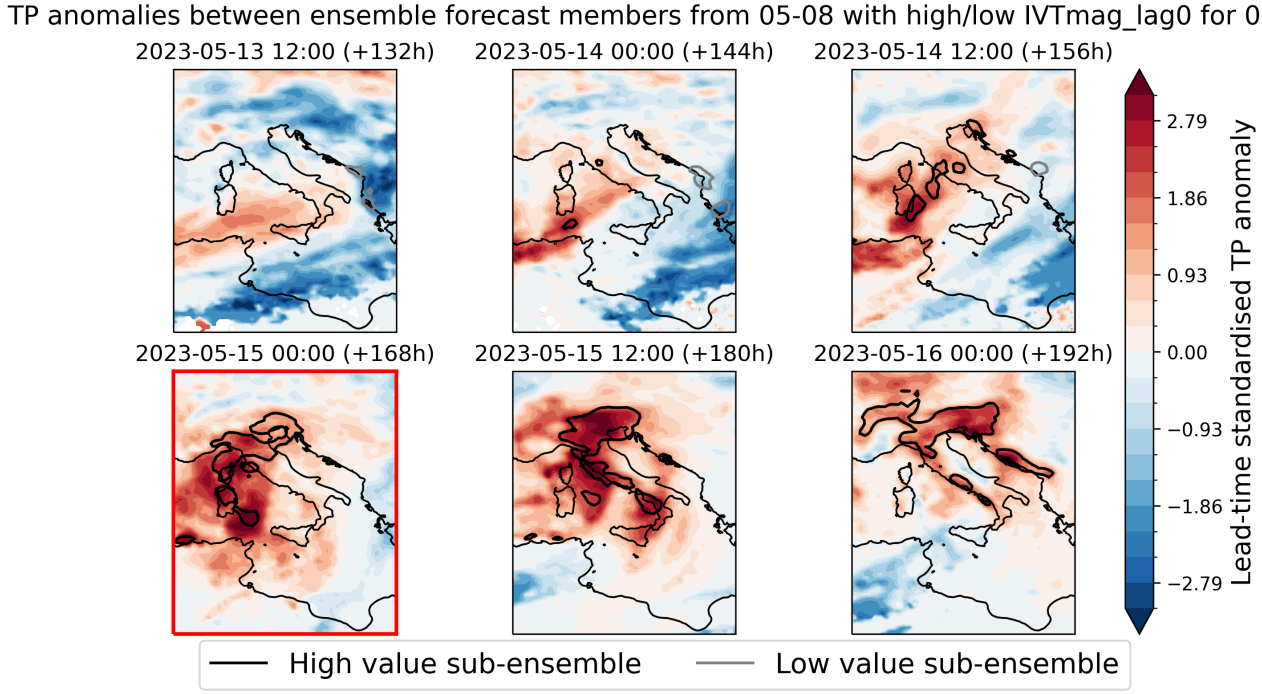

Figure S8. An ensemble sensitivity plot, as in figure 14 of the main text, but now showing total precipitation fields, rather than Z500.

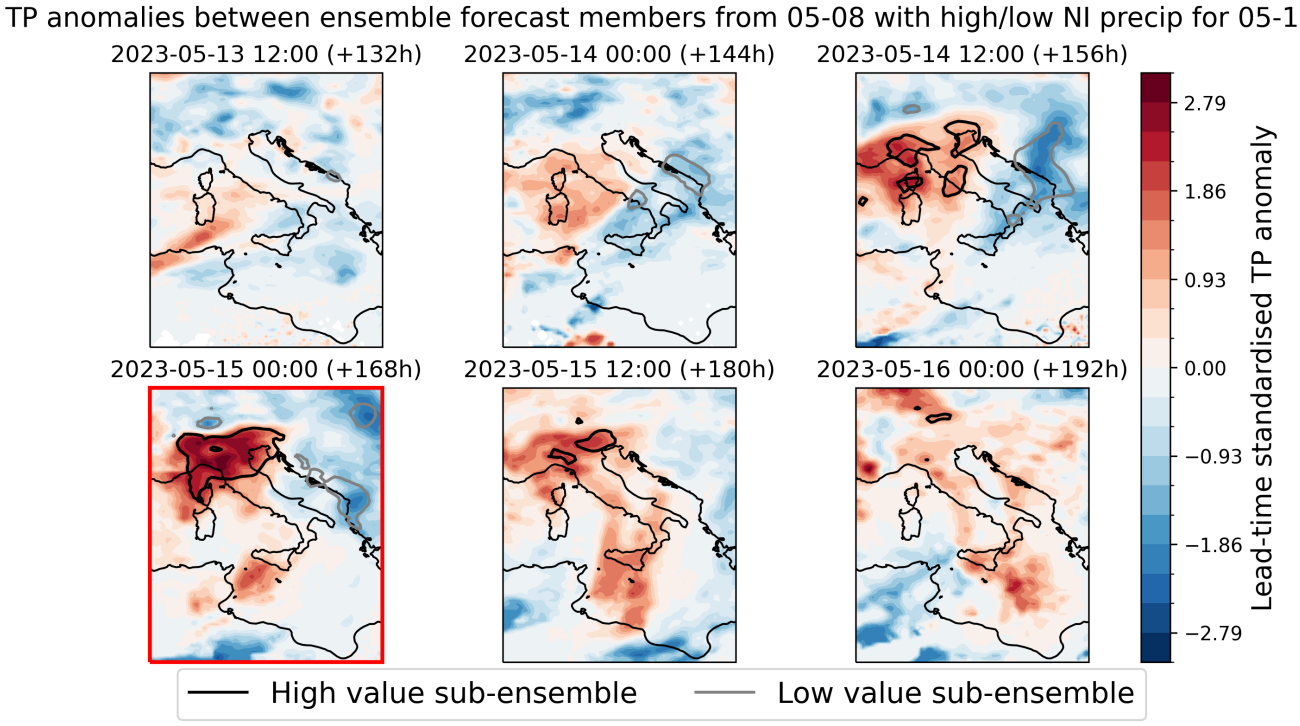

Figure S9. An ensemble sensitivity plot, as in figure 15 of the main text, but now showing total precipitation fields, rather than Z500.

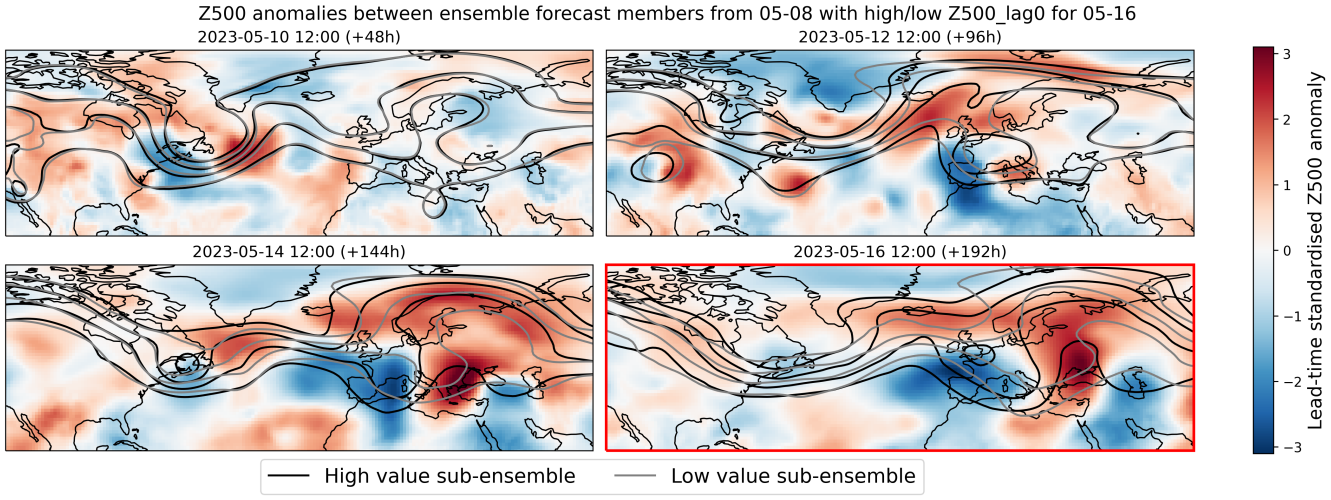

Figure S10. Ensemble sensitivity showing mean Z500 fields for two sub-ensembles of the 08/05/2023 forecast. sub-ensembles were defined by selecting the 5 ensemble members with the highest/lowest predicted values for the lag 0 Z500 precursor activity index on 16/05/2023.

S2 Supplementary Sensitivity Analyses

Here we include some brief discussion of two other sensitivity analyses based on the forecast evolution plots shown in main figure 13:

S2.1 Z500 precursor sensitivity from the 8th for the 16th

In the main text we show sensitivity plots of the forecast from 08/05 based on the value of the IVTmag lag 0 precursor on 15/05. Now we show sensitivity plots based on the Z500 lag 0 precursor on 16/05, due to the large uncertainty in Z500 precursors in that forecast.

In the Z500 field (Fig. S10), we see similar details as in the main text: uncertainty in trough position on the 10th affecting downstream ridge development, and so a stronger or weaker ridge-trough setup over Italy, in this case on the 16th. IVTmag fields (Fig. S11), show that in fact both high and low sub-ensembles show high IVTmag in the Mediterranean: in the high case, this is focused on the Adriatic and mirrors the development of Minerva, while in the low case, the IVTmag progresses East and predicts high transport over Greece. We therefore see that the sensitivity plots can provide some useful understanding of conditionality of possible extremes. While the large-scale flow in the high ensemble is close to what was observed in the case study, we see further evidence that the actual rainfall prediction itself is still imperfect in Fig. S12: rainfall is predicted for the 14th in the high value sub-ensemble, representing an overly fast propagation of the cyclone.

Conditioning on total precipitation, rather than Z500 precursors produces good discrimination of rainfall on the 16th, by construction (c.f. Fig S15). However, as in the main text, it is difficult to interpret a clear source of error in this case, and the coherence of the IVT scenarios is reduced (c.f. S13 and S14).

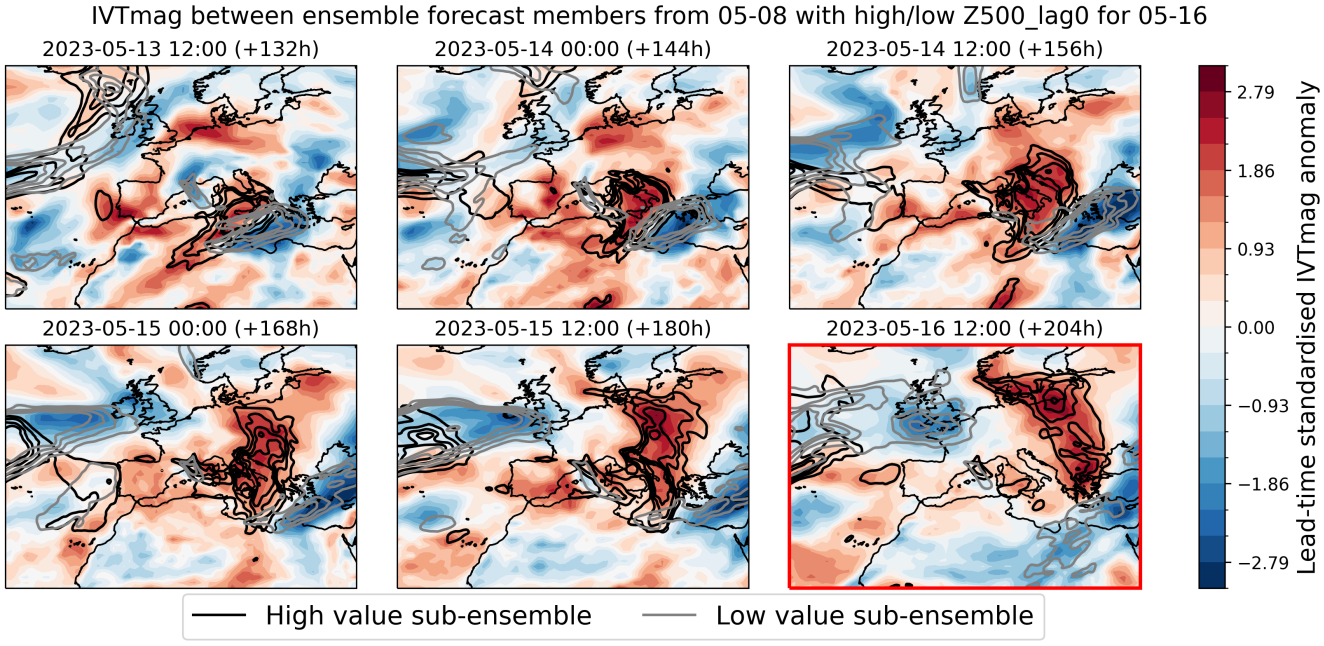

Figure S11. Ensemble sensitivity showing mean IVTmag fields for two sub-ensembles of the 08/05/2023 forecast. sub-ensembles were defined by selecting the 5 ensemble members with the highest/lowest predicted values for the lag 0 Z500 precursor activity index on 16/05/2023.

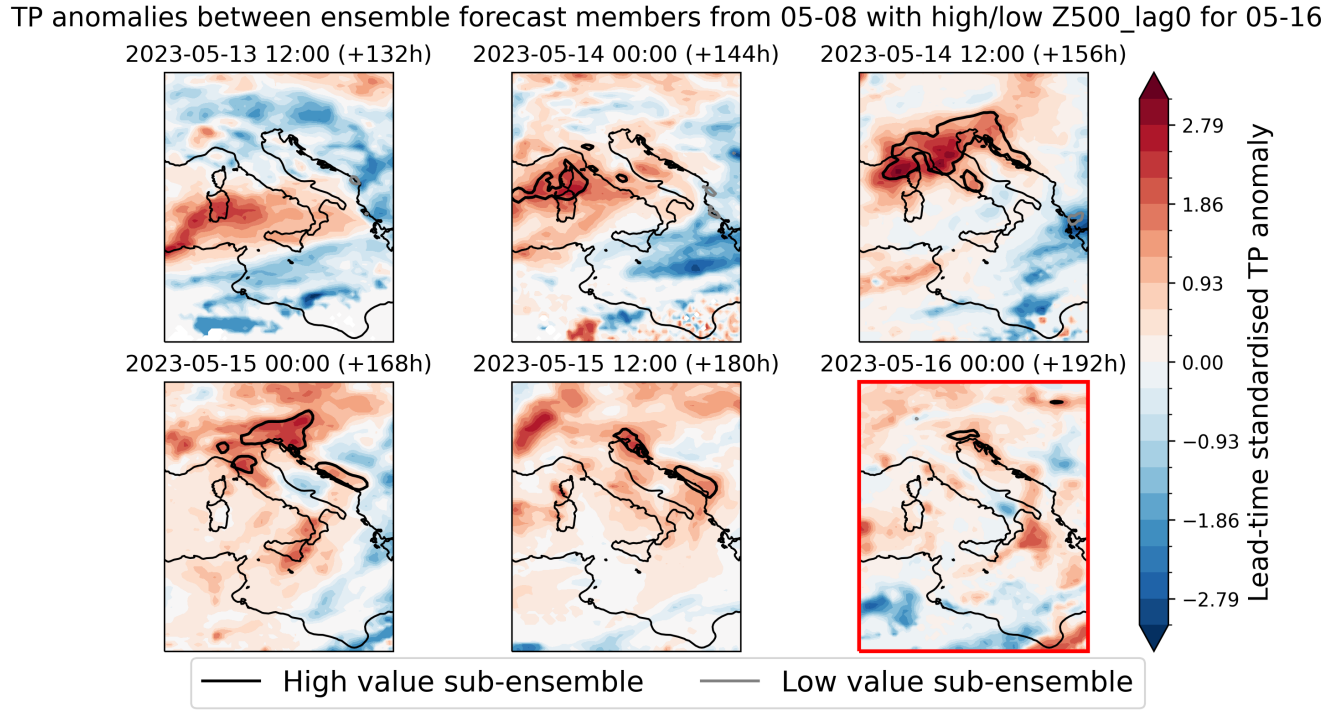

Figure S12. Ensemble sensitivity showing mean total precipitation fields for two sub-ensembles of the 08/05/2023 forecast. sub-ensembles were defined by selecting the 5 ensemble members with the highest/lowest predicted values for the lag 0 Z500 precursor activity index on 16/05/2023.

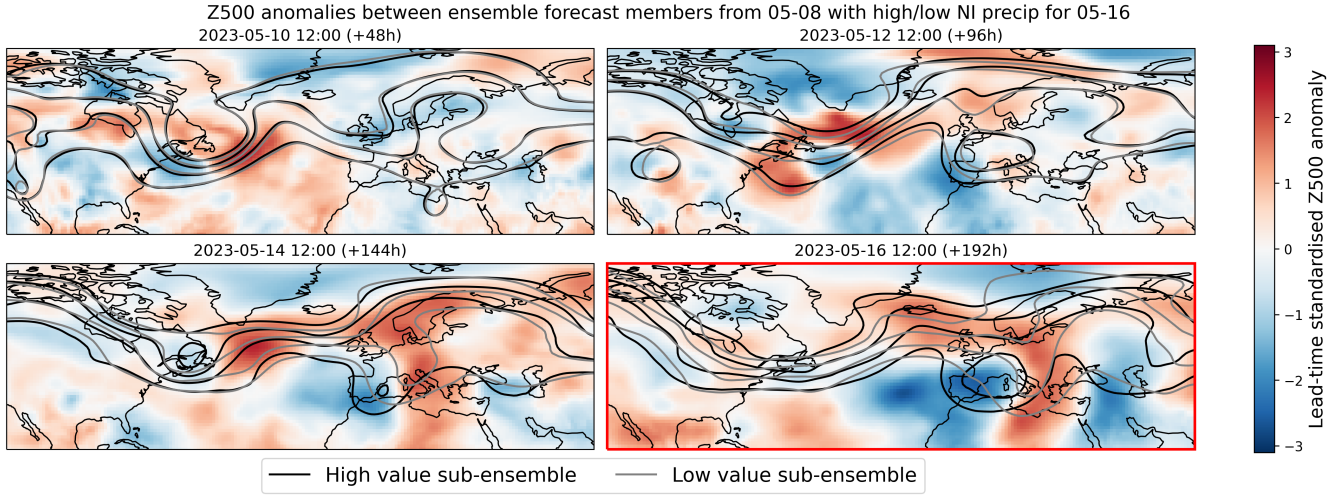

Figure S13. Ensemble sensitivity showing mean Z500 fields for two sub-ensembles of the 08/05/2023 forecast. sub-ensembles were defined by selecting the 5 ensemble members with the highest/lowest predicted values for north Italian total precipitation on 16/05/2023.

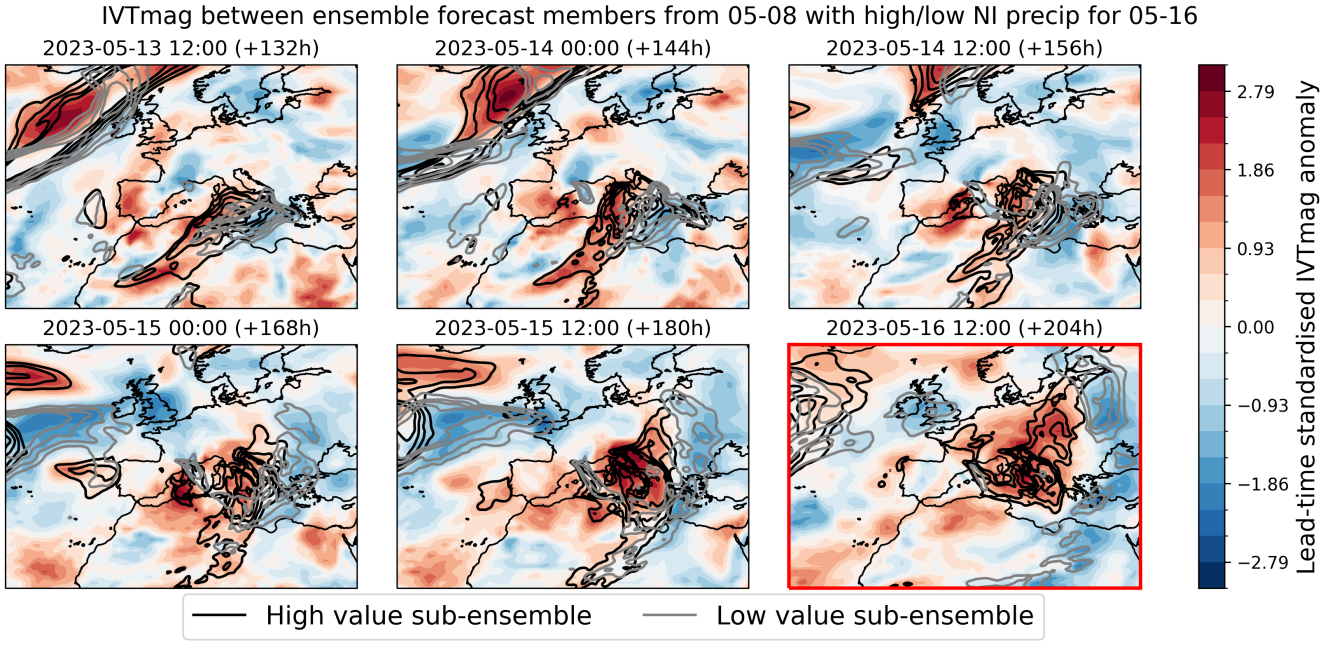

Figure S14. Ensemble sensitivity showing mean IVTmag fields for two sub-ensembles of the 08/05/2023 forecast. sub-ensembles were defined by selecting the 5 ensemble members with the highest/lowest predicted values for north Italian total precipitation on 16/05/2023.

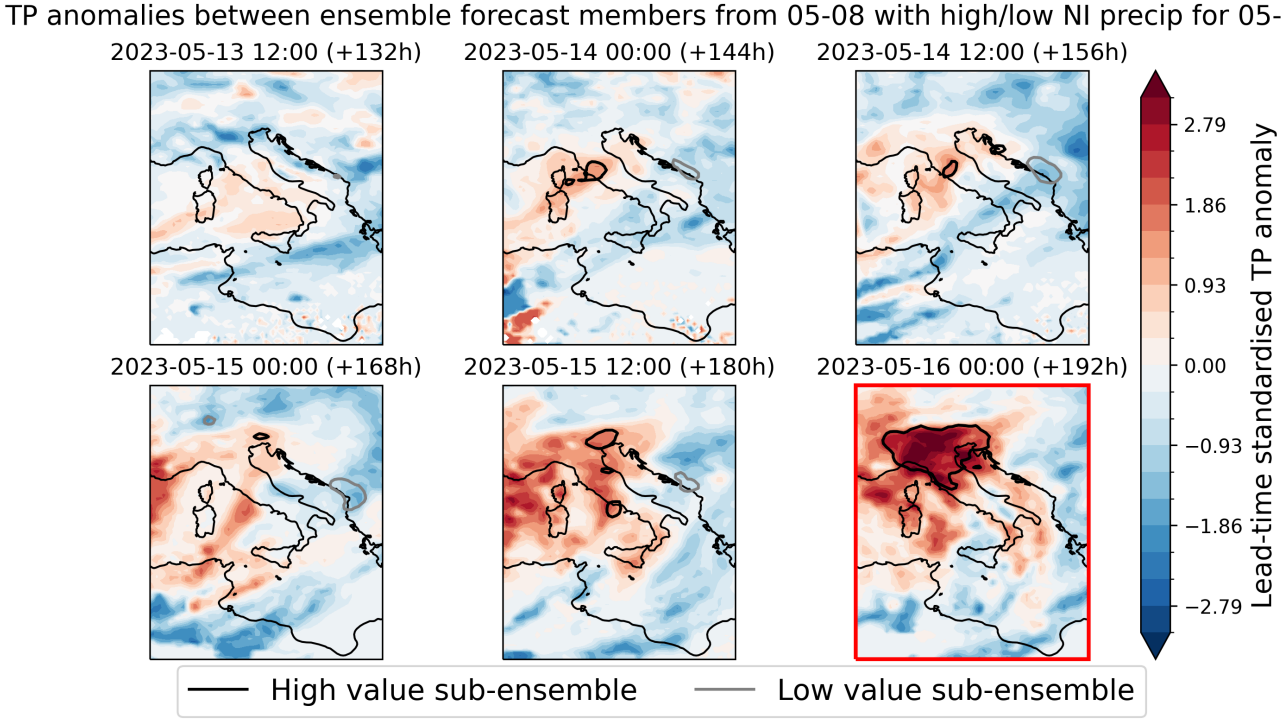

Figure S15. Ensemble sensitivity showing mean total precipitation fields for two sub-ensembles of the 08/05/2023 forecast. sub-ensembles were defined by selecting the 5 ensemble members with the highest/lowest predicted values for north Italian total precipitation on 16/05/2023.

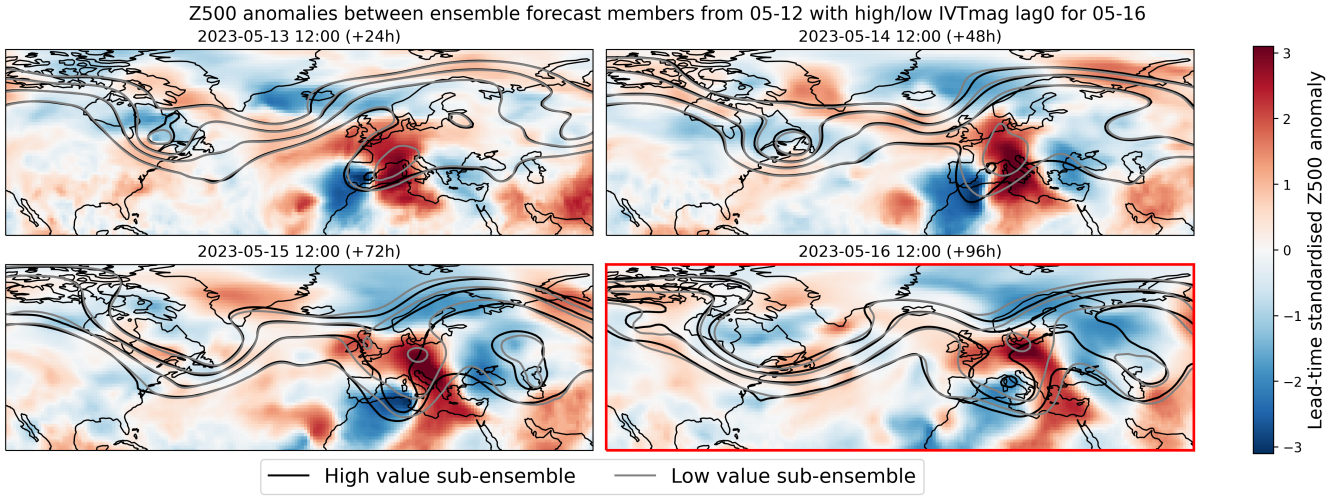

Figure S16. Ensemble sensitivity showing mean Z500 fields for two sub-ensembles of the 12/05/2023 forecast. sub-ensembles were defined by selecting the 5 ensemble members with the highest/lowest predicted values for IVTmag lag 0 precursor activity indices on 16/05/2023.

S2.2 IVTmag precursor sensitivity from the 12th for the 16th

As a final example sensitivity analysis, we consider a shorter range forecast, looking at the forecast from the 12th, conditioned on IVTmag lag 0 precursor activity for the 16th. This forecast represented a large jump in ensemble mean IVTmag predictions and a skew towards high rainfall scenarios, but still with substantial uncertainty.

From figure S16 we clearly see that this short-range uncertainty came down to the exact shape and tilt of the cutoff low over Europe, and so is a direct result of the increased flow instability associated with the cyclonic wavebreaking. To emphasise: the previous considered sensitivity plots showed uncertainty in whether the wave would break based on Labrador sea cyclone development, while here we see uncertainty in *how* the wave breaks. This provides two different predictability barriers, with qualitative, probabilistic information after the first is crossed, and increasingly deterministic and small-scale information after the second is crossed.

The result of the different position of the cut-off low, is an alteration in the cyclone track, which features a stronger westerly component in the low IVTmag members (c.f.S17), which leads to strong rainfall over Albania, and a wider band of weak rainfall over Eastern Europe (c.f.S18). The high IVT members confine high IVT to the Adriatic and Tyrrhenian seas and predict north Italian rainfall on the 15th and 16th.

At this shorter lead time, sensitivity plots based on the direct precipitation forecast become a bit more useful and intepretable (figures S19-S21), but still show reduced discrimination in the large-scale flow, and it is still less easy to attribute divergence to spatially localised uncertainty. Here the precipitation fields show that the forecast was still predicting rainfall too early, with heavy rain focused early on the 15th.

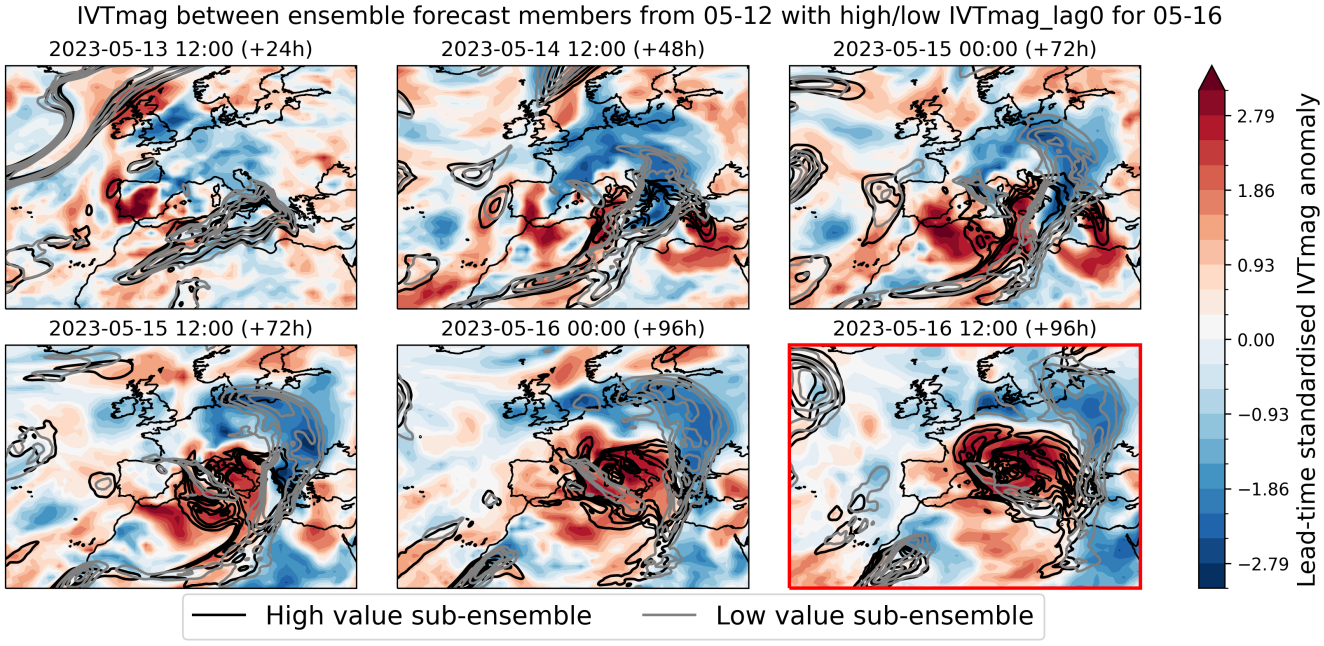

Figure S17. Ensemble sensitivity showing mean IVTmag fields for two sub-ensembles of the 12/05/2023 forecast. sub-ensembles were defined by selecting the 5 ensemble members with the highest/lowest predicted values for IVTmag lag 0 precursor activity indices on 16/05/2023.

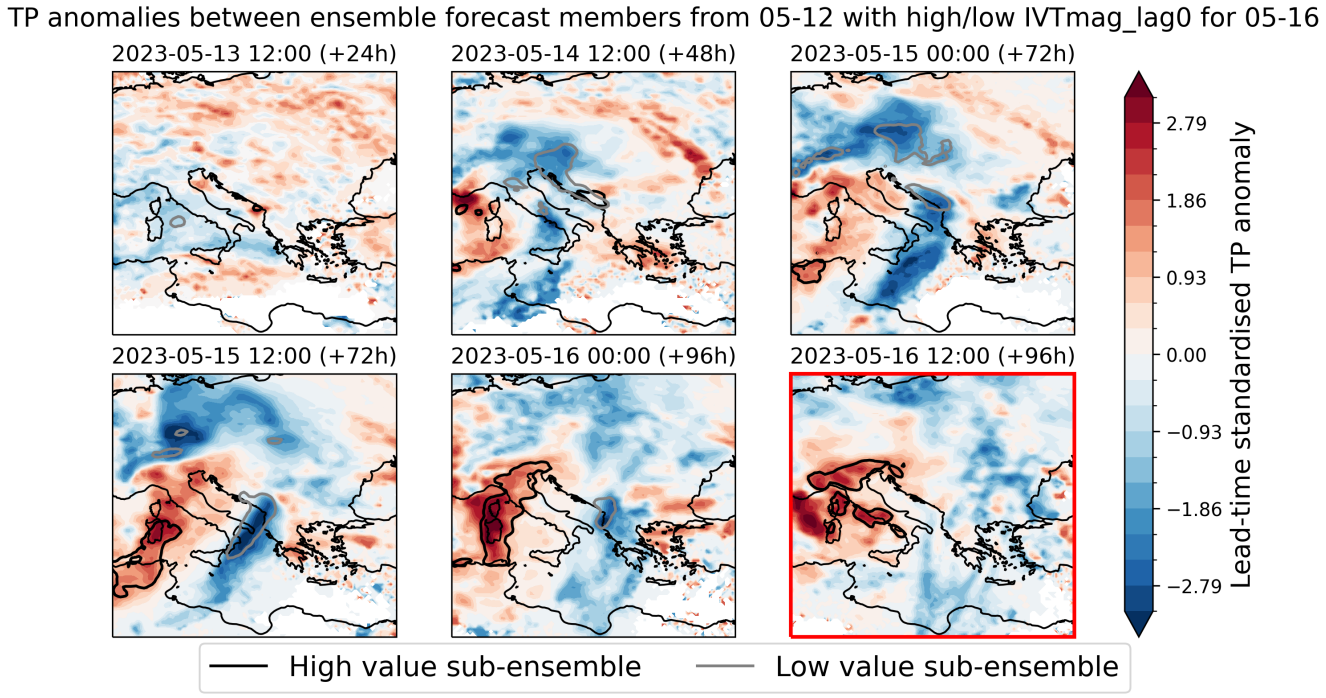

Figure S18. Ensemble sensitivity showing mean total precipitation fields for two sub-ensembles of the 12/05/2023 forecast. sub-ensembles were defined by selecting the 5 ensemble members with the highest/lowest predicted values for IVTmag lag 0 precursor activity indices on 16/05/2023.

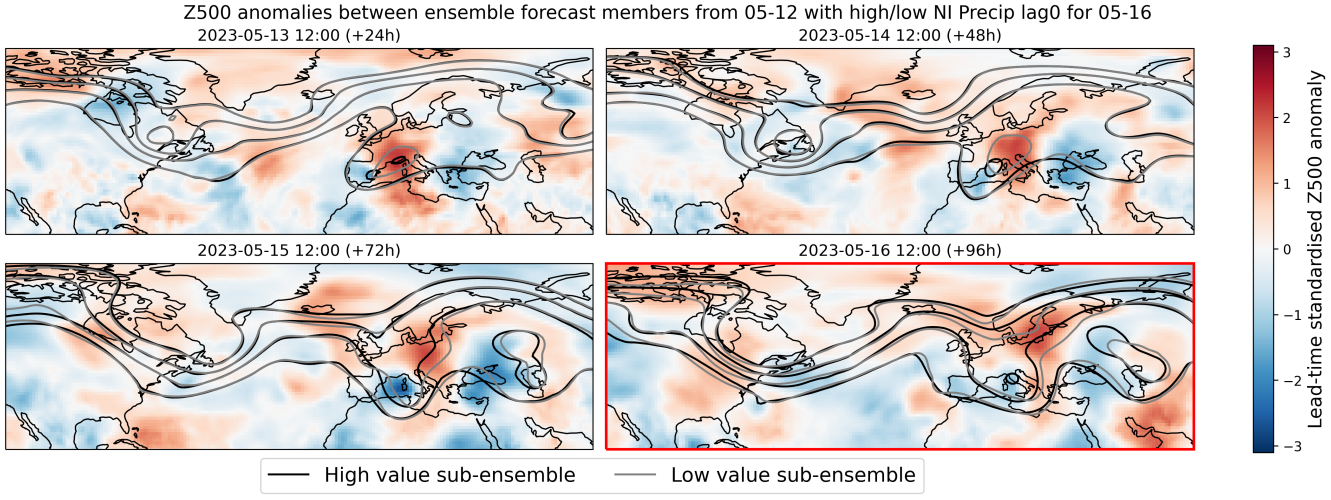

Figure S19. Ensemble sensitivity showing mean Z500 fields for two sub-ensembles of the 12/05/2023 forecast. sub-ensembles were defined by selecting the 5 ensemble members with the highest/lowest predicted values for north Italian total precipitation on 16/05/2023.

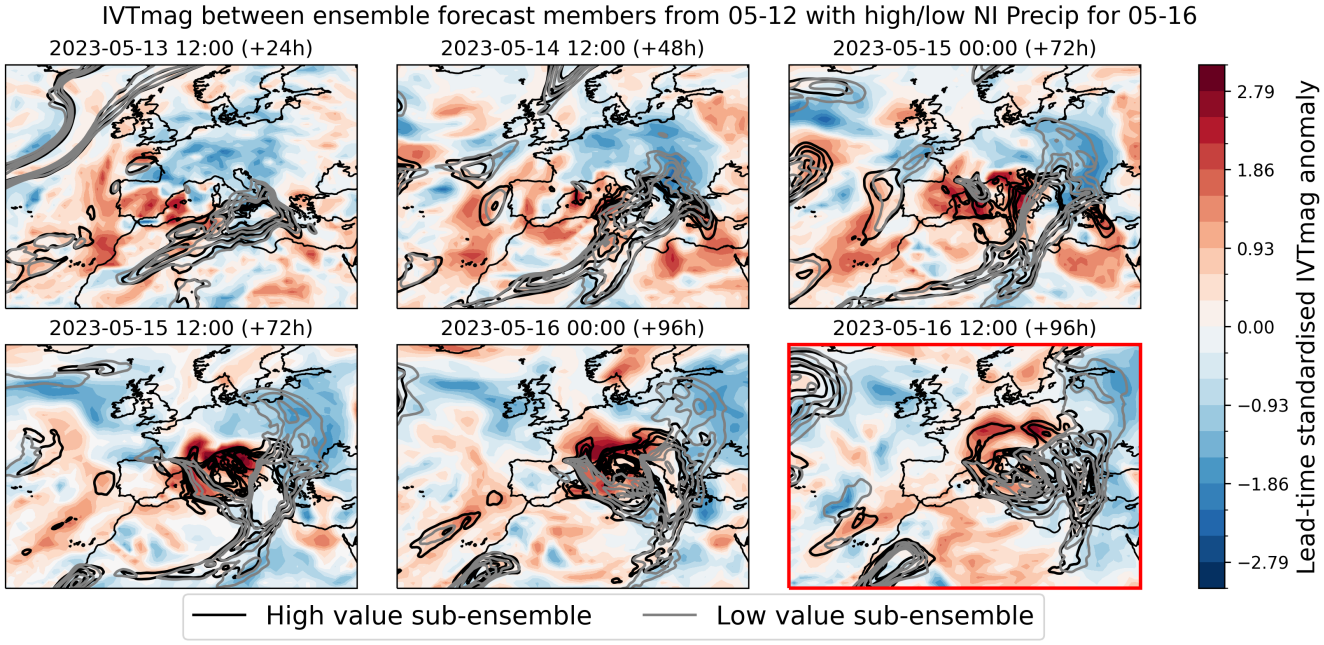

Figure S20. Ensemble sensitivity showing mean IVTmag fields for two sub-ensembles of the 12/05/2023 forecast. sub-ensembles were defined by selecting the 5 ensemble members with the highest/lowest predicted values for north Italian total precipitation on 16/05/2023.

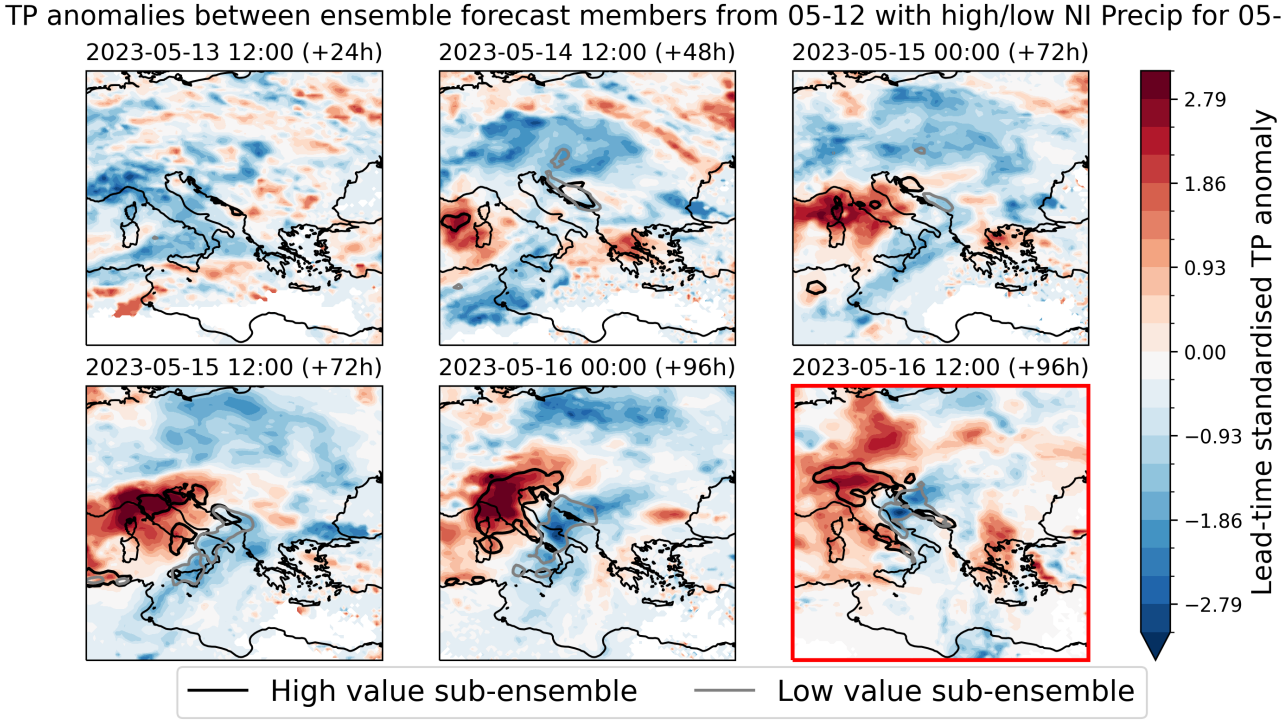

Figure S21. Ensemble sensitivity showing mean total precipitation fields for two sub-ensembles of the 12/05/2023 forecast. sub-ensembles were defined by selecting the 5 ensemble members with the highest/lowest predicted values for north Italian total precipitation on 16/05/2023.